

Nanothermoforming of hierarchical optical components utilizing shape memory polymers as active molds

Norbert Schneider,¹ Claudia Zeiger,¹ Alexander Kolew,¹ Marc Schneider,¹ Juerg Leuthold,^{1,2} Hendrik Hölscher,^{1,*} Matthias Worgull¹

¹Institute of Microstructure Technology (IMT), Karlsruhe Institute of Technology (KIT), Hermann-von-Helmholtz-Platz 1, 76344 Eggenstein-Leopoldshafen, Germany

²Institute of Electromagnetics and Photonics (IFH), ETH Zürich, Gloriastrasse 35, 8092 Zürich, Switzerland

*Hendrik.Hoelscher@kit.edu

Abstract: We utilize shape memory polymers as active mold inserts for the thermoforming of complex, hierarchical nano- and microstructured optical components with undercuts on large scales. Our approach combines nanoimprint/hot embossing and thermoforming with the unique features of shape memory polymers. As examples for this nano- and microthermoforming process, we demonstrate the fabrication of hierarchical photonic structures inspired by the blue *Morpho* butterfly as well as diffractive optical elements with nm- and μm -size structures.

© 2014 Optical Society of America

OCIS codes: (220.4241) Nanostructure fabrication; (220.4000) Microstructure fabrication; (160.1245) Artificially engineered materials.

References and links

1. C. G. Bernhard, "Structural and functional adaptation in a visual system," *Endeavour* **26**, 79–84 (1967).
2. A. R. Parker, "515 million year of structural colors," *J. Opt. A: Pure Appl. Opt.* **2**, R15–R28 (2000).
3. P. Vukusic and J. R. Sambles, "Photonic structures in biology," *Nature* **424**, 852–855 (2003).
4. R. A. Potyrailo, H. Ghiradella, A. Vertiatchick, K. Dovidenko, J. R. Cournoyer, and E. Olson, "Morpho butterfly wing scales demonstrate highly selective vapor response," *Nature Photonics* **1**, 123–128 (2007).
5. L. Biro and J. Vigneron, "Photonic nanoarchitectures in butterflies and beetles: valuable sources for bioinspiration," *Laser & Photon. Rev.* **5**, 27–51 (2011).
6. D. G. Stavenga, S. Foletti, G. Palasantzas, and K. Arikawa, "Light on the moth-eye corneal nipple array of butterflies," *Proc. R. Soc. B* **273**, 661–667 (2006).
7. A. Gombert, W. Glaubitt, K. Rose, J. Dreiholz, B. Bläsi, A. Heinzel, D. Sporn, W. Döll, and V. Wittwer, "Subwavelength-structured antireflective surfaces on glass," *Thin Solid Films* **351**, 73–78 (1999).
8. Y.-F. Huang, S. Chattopadhyay, Y.-J. Jen, C.-Y. Peng, T.-A. Liu, Y.-K. Hsu, C.-L. Pan, H.-C. Lo, C.-H. Hsu, Y.-H. Chang, C.-S. Lee, K.-H. Chen, and L.-C. Chen, "Improved broadband and quasi-omnidirectional anti-reflection properties with biomimetic silicon nanostructures," *Nature Nanotechnology* **2**, 770–774 (2007).
9. A. D. Pris, Y. Utturkar, C. Surman, W. G. Morris, A. Vert, S. Zalyubovskiy, T. Deng, H. T. Ghiradella, and R. A. Potyrailo, "Towards high-speed imaging of infrared photons with bio-inspired nanoarchitectures," *Nature Photonics* **6**, 195–200 (2012).
10. S. J. Abbott and P. H. Gaskell, "Mass production of bio-inspired structured surfaces," *Proc. IMechE Vol. 221C* **221**, 1181–1191 (2007).
11. M. Worgull, *Hot Embossing - Theory and Technology of Microreplication* (William Andrew, 2009), 1st ed.
12. E. Brousseau, S. Dimov, and D. Pham, "Some recent advances in multi-material micro- and nano-manufacturing," *Int. J. Adv. Manuf. Technol.* **47**, 161–180 (2010).
13. M. Aryal, D.-H. Ko, J. R. Tumbleston, A. Gadisa, E. T. Samulski, and R. Lopez, "Large area nanofabrication of butterfly wing's three dimensional ultrastructures," *J. Vac. Sci. Technol. B* **30**, 061802 (2012).
14. N. C. Lee, *Understanding Blow Molding* (Hanser-Gardner Publ., 2007), 2nd ed.

15. M. Heilig, S. Giselbrecht, A. Guber, and M. Worgull, "Microthermoforming of nanostructured polymer films: a new bonding method for the integration of nanostructures in 3-dimensional cavities," *Microsys. Technol.* **16**, 1221–1231 (2010).
16. M. Heilig, M. Schneider, H. Dingreiter, and M. Worgull, "Technology of microthermoforming of complex three-dimensional parts with multiscale features," *Microsys. Technol.* **17**, 593–600 (2011).
17. R. Truckenmueller, Z. Rummeler, T. Schaller, and W. K. Schomburg, "Low-cost thermoforming of micro fluidic analysis chips," *J. Micromech. Microeng.* **12**, 375 (2002).
18. S. Giselbrecht, T. Gietzelt, E. Gottwald, C. Trautmann, R. Truckenmüller, K. Weibezahn, and A. Welle, "3d tissue culture substrates produced by microthermoforming of pre-processed polymer films," *Biomed. Microdevices* **8**, 191–199 (2006).
19. A. Lendlein and R. Langer, "Biodegradable, elastic shape-memory polymers for potential biomedical applications," *Science* **296**, 1673–1676 (2002).
20. C. Liu, H. Qin, and P. T. Mather, "Review of progress in shape-memory polymers," *J. Mat. Chem.* **17**, 1543–1558 (2007).
21. T. Xie, "Tunable polymer multi-shape memory effect," *Nature* **464**, 267–270 (2010).
22. M. Behl, M. Y. Razzaq, and A. Lendlein, "Multifunctional Shape-Memory Polymers," *Adv. Mater.* **22**, 3388–3410 (2010).
23. H. Xu, C. Yu, S. Wang, V. Malyarchuk, T. Xie, and J. A. Rogers, "Deformable, Programmable, and Shape-Memorizing Micro-Optics," *Adv. Func. Mat.* **23**, 3299–3306 (2013).
24. A. Espinha, M. C. Serrano, Á. Blanco, and C. López, "Thermoresponsive Shape-Memory Photonic Nanostructures," *Adv. Optical Mater.* pp. 516–521 (2014).
25. E. W. Becker, W. Ehrfeld, P. Hagmann, A. Maner, and D. Münchmeyer, "Fabrication of microstructures with high aspect ratios and great structural heights by synchrotron radiation lithography, galvanofarming, and plastic molding (LIGA process)," *Microelectron. Eng.* **4**, 35–56 (1986).
26. L. J. Guo, "Nanoimprint lithography: Methods and material requirements," *Adv. Mater.* **19**, 495–513 (2007).
27. H. Schiff and A. Kristensen, *Handbook of Nanotechnology* (Springer Verlag, Berlin, 2010), chap. 9. Nanoimprint lithography - Patterning of Resists Using Molding, pp. 271–312, 3rd ed.
28. H. Kikuta, H. Toyota, and W. Yu, "Optical elements with subwavelength structured surfaces," *Opt. Rev.* **10**, 63–73 (2003).
29. A. Waddie, M. Taghizadeh, J. Mohr, V. Piottter, C. Mehne, A. Stuck, E. Stijns, and H. Thienpont, *Design, fabrication and replication of micro-optical components for educational purposes within the Network of Excellence in Micro-Optics (NEMO)*, SPIE Proceedings Vol. 6185, doi:10.1117/12.661912 (2006).
30. C. Stuart and Y. Chen, "Roll in and roll out: A path to high-throughput nanoimprint lithography," *ACS Nano* **3**, 2062–2064 (2009).

1. Introduction

Many optical structures found in nature offer a variety of interesting and useful features originating from their nanostructure [1–5]. Nanonipples on the moth eye, for example, dramatically decrease its reflectivity [1, 6] and inspired the design of anti-reflex coatings [7, 8]. Various butterflies generate their colorful appearance through structural colors [2, 3] and the Christmas tree-like structure of the famous blue *Morpho* butterflies inspired new concepts for sensors [4, 9]. However, commercial applications of these bio-inspired optical components rely on large scale production techniques to be cost effective [10]. Morphologies like the moth eye can be easily replicated as there are no undercuts [11, 12]. Truly three-dimensional nanostructures with undercuts like the Christmas tree-like structure of the *Morpho* butterfly, however, are still a challenge which can be attacked by material specific under-etching [13]. Nonetheless, the replication of complex, hierarchical nano- and microstructures is laborious and restricted to small areas in many cases. Therefore, it is of high interest to develop new processes for the production of optical components on large scales.

One approach to manufacture macroscopic structures of higher complexity without detriment concerning the area is thermoforming or blow-molding, usually employed for industrial shaping of polymers at low costs [11, 14]. This manufacturing approach can be downsized and reaches smaller dimensions using microthermoforming [15, 16]. Microfluidic devices can be thermoformed from previously processed polymer foils to replicate three dimensional structures [17, 18]. This combination of structuring and subsequent thermoforming of a polymer foil

allows the three-dimensional fabrication on large areas. Nevertheless, the route from micro- to nanoscale thermoforming is blocked by several issues. The fundamental principle of thermoforming requires that the thickness of the polymer foil is less than half the size of the smallest cavity to be filled. Therefore, the thickness of the foil has to decrease with structure size. Polymer foils with a thickness of some hundreds of nanometers, however, are not mechanically stable enough to survive uneven stretching during thermoforming and release from the mold after thermoforming. Consequently, a simple downscaling of this approach towards optical nanostructures is not within reach.

To overcome these issues we utilize shape memory polymers (SMPs) [19–22] as active mold inserts for the thermoforming of complex, hierarchical nano- and microstructures which can be used as optical components. It is a remarkable ability of SMPs to recover from a temporary shape to a previously defined, permanent shape by an external stimulus like heat. A thermoresponsive SMP, for example, is processed above its permanent temperature T_{perm} to receive the permanent shape. After subsequent deformation at lower temperatures it recovers (or "remembers") this shape if heated above its transitions temperature T_{trans} [19]. The implementation of a SMP into an established large area replication process allows us to bypass limitations unavoidable in classical thermoforming and paves the way to fabricate optical components with hierarchical features on large areas. In this way we expand recent studies on optical components produced from SMPs without hierarchy [23, 24]. We demonstrate the basic principle of nanothermoforming with SMPs by the manufacturing of photonic structures inspired by the blue Morpho butterfly and the composition of diffractive optical elements.

2. Experimental

2.1. Nanothermoforming with shape memory polymers

The final structures produced by nanothermoforming have primary (typically μm) features imposed by the structure of a shape memory polymer and secondary (typically nm) features on a thin polymer film covering the SMP. As shown in Fig. 1, the primary structure is defined by hot embossing [11, 25] – also known as thermal nanoimprint (NI) [26, 27] – into the SMP and this process consists of three basic steps. As SMP we used an aromatic polyether-based thermoplastic polyurethane (Tecoplast[®] TP-470, Lubrizol) with a $T_{\text{perm}} \approx 170^\circ\text{C}$ and $T_{\text{trans}} \approx 80^\circ\text{C}$. In the first step, a $500\ \mu\text{m}$ -thick SMP foil is placed between a mold insert and a counter plate. This setup is contained within an evacuated chamber ensuring a complete filling of cavities and preventing an uncontrolled heating due to the compression of air in cavities [11]. The sample is heated to a defined temperature above the SMP's permanent shaping temperature. In the second step, a force is applied to the substrate and the SMP is pressed into the cavities. A sufficient holding time is kept to allow the polymer mold to fill the cavities of the mold insert completely. In the third step, the SMP cooled down to room temperature while the previously applied force is kept constant to compensate for polymer shrinkage [11]. In this embossing step we applied a temperature of 200°C with a pressure of 3 MPa. In a second embossing process, the structures are temporarily flattened using a flat plate instead of a structured mold insert. The temperature for this step is chosen to ease the process by lowering the SMP's viscosity but still it has to remain under T_{perm} to ensure a temporary flattening only. In our case, the embossing temperature is set to 90°C while a pressure of 3-4 MPa is applied. During the following processing steps we use this programmed SMP as an active mold insert.

In order to embed the secondary (or nano-scale) structure, a thin polymer film is spin-coated onto the flat SMP which now acts as a substrate. For the presented examples, we created a polymethyl methacrylate (PMMA, Allresist AR-P-672) film with thicknesses between 100 nm and $1\ \mu\text{m}$. In contrast to common spin-coating, we omit the post-baking step in order to prevent the SMP from recovering prematurely. To compensate for this, we keep the spin-coated samples

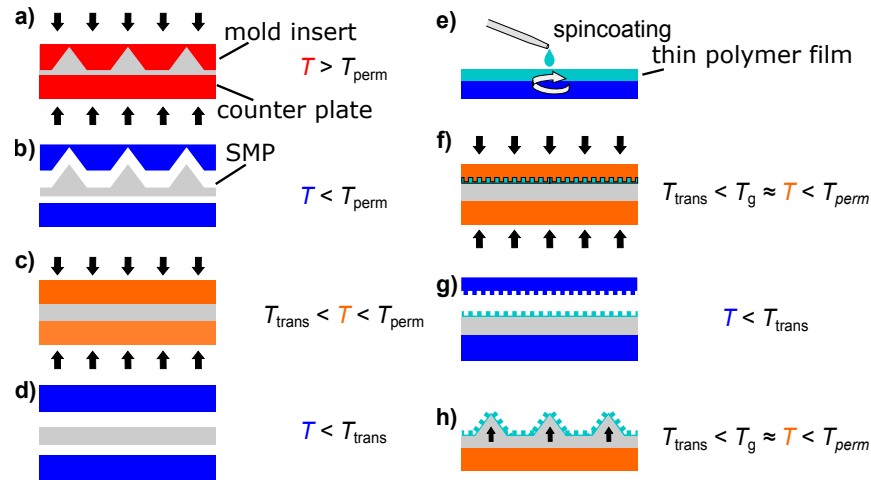


Fig. 1. Schematic of the hierarchical nano- and microthermoforming of optical component with a shape memory polymer (not to scale). (a) A primary structure is permanently replicated into a SMP foil by hot embossing with a mold insert, (b) then demolded and (c+d) hot embossed again to a temporary flat shape. (e) Afterwards, an ultrathin polymer layer is spincoated onto the flat SMP and (f+g) hot embossed with the secondary structure. (h) Finally, both polymer films are heated and the thin nanostructured film is thermoformed by the recovering of the SMP into its permanent shape. As described in the text this is the important step for the fabrication of hierarchical structures and the relation between the characteristic temperatures of the SMP (T_{perm} , T_{trans}) and the thin film (T_g) is crucial for it.

at room temperature for an accordingly long period (12–16 h) to ensure a proper diffusion of the solvent. (This process time can be reduced to 1 hour by drying in vacuum to accelerate evaporation of the solvent.) The next step comprises the embossing of the previously spincoated polymer film, thus generating the secondary structure. The embossing is performed in the same way as the hot embossing of the SMP. The choice of the embossing temperature, however, is crucial during this process step. It has to be well below the permanent shaping temperature T_{perm} of the SMP to preserve the pre-structured pattern of the active mold insert and above the glass transition temperature of the spincoated polymer film ($T_g = 105^\circ\text{C}$ for PMMA). Being limited to low temperatures by these constraints, the thin polymer film might be embossed with higher pressures if required.

In the final step of the process, we heat the whole sample above the transition temperature of the SMP to 100°C near to the glass transition temperature of the polymer film. Since a shape memory polymer recovers its permanent shape if it is heated above its transition temperature, the polymer film on its surface is thermoformed by the restoring force of the SMP. Near its glass temperature the polymer still remains in a rubber-elastic state [15] and this choice allows an easier shaping of the film but preserves the polymeric structure as well as the embossed nanostructures on its surface. The surface structures remain intact due to the choice of temperature, but they are widened due to the stretching by the SMP. The final step (Fig. 1h) is different to conventional thermoforming because the spincoated polymer layer containing the secondary structure is formed into its final shape by the underlying SMP and not by gas pressure, i.e., the shape memory polymer acts as an active mold. After the complete recovery of the SMP, the setup is cooled down to room temperature to avoid further deformations during subsequent handling. The final sample features the thermoformed primary structure of the SMP as well as the embossed secondary structures on its surface.

2.2. Examples

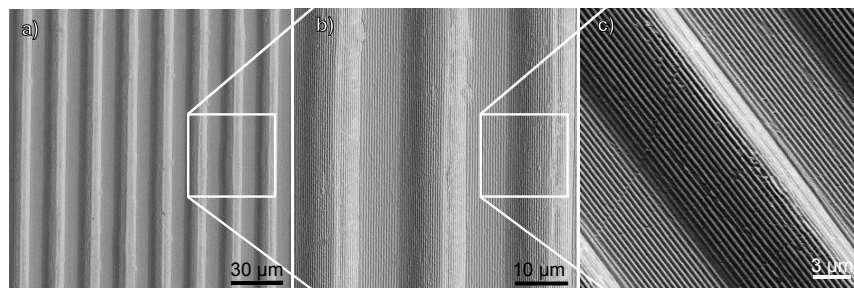


Fig. 2. SEM images of a triangular grating with a period $20\ \mu\text{m}$ superimposed with a $400\ \text{nm}$ grating manufactured using the process described in Fig. 1. (a) The overview demonstrates the uniformity whereas (b) presents details of the structured surface. The $400\ \text{nm}$ grating remained intact during the nanothermoforming process. (c) The tilted view into the secondary structures reveals the distinctive undercuts created by the $400\ \text{nm}$ grating on the slopes of the underlying triangular ridges.

Applying the above described manufacturing steps, we fabricated a surface with triangular shaped ridges superimposed with a grating of $400\ \text{nm}$ period (see Fig. 2). The triangular primary structures were replicated into the $500\ \mu\text{m}$ -thick SMP film and as previously described we spincoated a $110\ \text{nm}$ film of PMMA on top. The primary as well as the secondary structure have an aspect ratio of about 1. As revealed by the tilted view displayed in Fig. 2c) the structures of the smaller grating appear as undercuts at the slopes of the ridges.

This approach also works on smaller scales as demonstrated by the example shown in Fig. 3. Here, we manufactured a photonic structure inspired by the famous blue *Morpho* butterfly [2, 3] and recorded the topography of the sample during the fabrication steps by atomic force microscopy (AFM). Compared with the first example, we used a denser grating with a period of $3\ \mu\text{m}$ to program the primary structure into the SMP sample. Applying now the same steps described above, we again define the secondary structure by a grating with a period of $400\ \text{nm}$. After heating the sample, the primary structure recovers and the surface features two gratings with different periods and the overall structure resembles that of the of the *Morpho* butterfly.

Consequently, the final sample shows the famous wide-angle iridescence for blue light and appears blue for viewing angles up to 15° while the $400\ \text{nm}$ grating is blue only for vertical incidence (see Fig. 3d). In order to quantify this effect in more detail we recorded optical spectra of both samples using a Perkin Elmer LAMBDA 1050 UV/Vis/NIR Spectrophotometer with integrating sphere. The integrated spectrum of the $400\ \text{nm}$ grating does not show pronounced features. The *Morpho*-type structure on the other hand has peaks in the blue color regime explaining its blue appearance for a wide range of angles.

During the transition of the SMP to its permanent shape the thin polymer film is stretched depending on the aspect ratio of the primary structure and the secondary structure embossed into this thin film is stretched accordingly. This effect has been taken into account for the final design of the hierarchical structure. Furthermore, the spincoated polymer foil (PMMA in our case) exerts a force onto the recovering SMP thus preventing a complete recovery of its initial shape. As shown in Fig. 3a) and c) the SMP consistently only recovers back to 35% of its initial height in our case. This value, however, might be larger or smaller depending on the actual geometry of the two structures as well as the material properties and thicknesses of the two films.

As both materials, the shape memory polymer Tecoplast as well as the PMMA, are transpar-

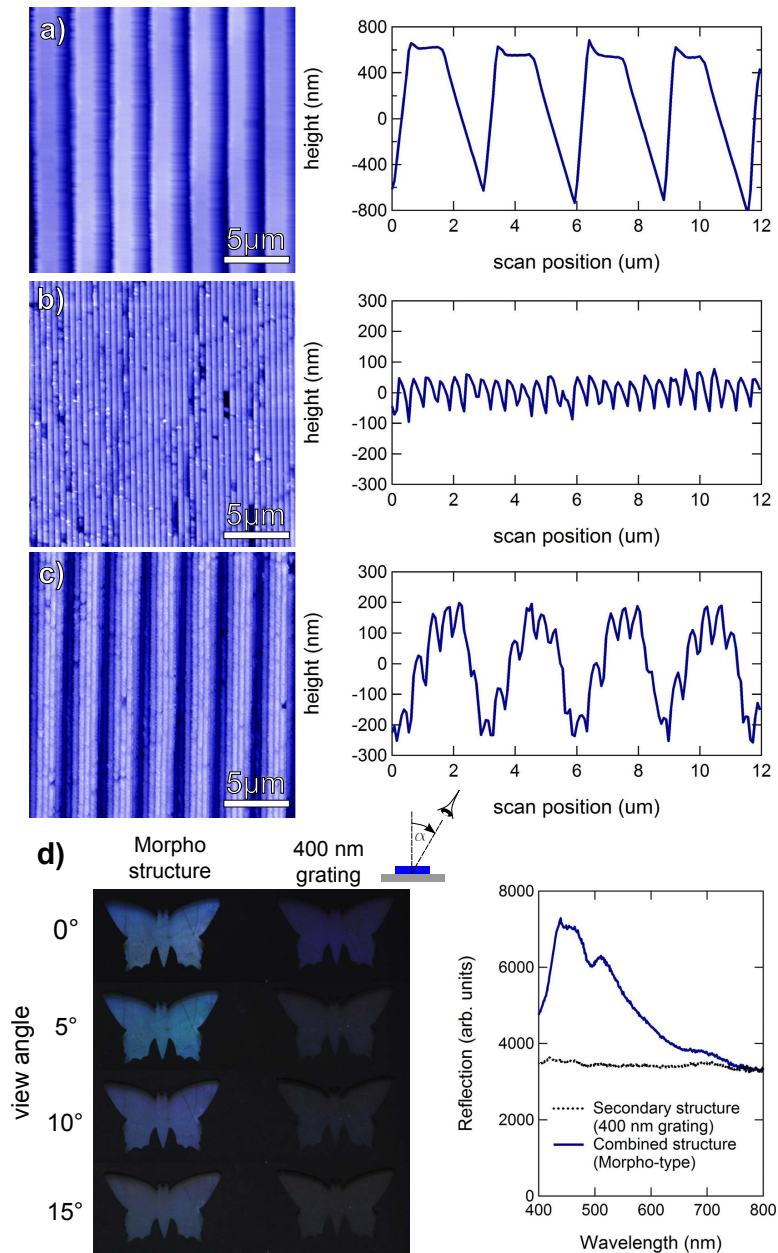


Fig. 3. Fabrication of a *Morpho*-type structure. The topography images (left) and line scans (right) of the samples were measured by atomic force microscopy. **(a)** The grating has a periodicity of 3 μm which is hot embossed into the shape memory polymer. Subsequently, the surface is flattened and a thin PMMA film is spin-coated onto the SMP. **(b)** The AFM image and line scan show the 400 nm grating which is hot embossed into the thin film. **(c)** Finally, after the recovery of the previously programmed primary structure both gratings are combined. The resulting surface topography resembles that of the optical structure of a *Morpho* butterfly. **(d)** A direct comparison of the 400 nm grating with the final *Morpho*-type structure in diffusive white light reveals that the blue iridescence of the butterfly structure appears blue even for large viewing angles of up to 15° while the 400 nm grating does not. The total reflection spectra of the 400 nm grating (dashed line) and the replicated *Morpho*-type structure (solid line) explain the difference in their optical appearance.

ent for visible wavelengths it is also possible to combine diffractive optical elements (DOE) [28] with our approach. Figure 4 shows the combination of two optical structures. The primary structure is a simple linear grating with a period of $3\ \mu\text{m}$ programmed into the SMP. The interference maxima of zero and first order can be observed when coherent light shines through the grating (Fig. 4a). As secondary structure we embossed a pattern forming diffractive optical element (PF-DOE) [29] into the thin PMMA film. This structure is the Fourier transform of a flattop [29] which appears on the screen (Fig. 4b). Heating now the sample above the transition temperature, the primary structure of the SMP recovers and the two structures can be observed as a combination on the screen as well as in the topography of the sample (Fig. 4c).

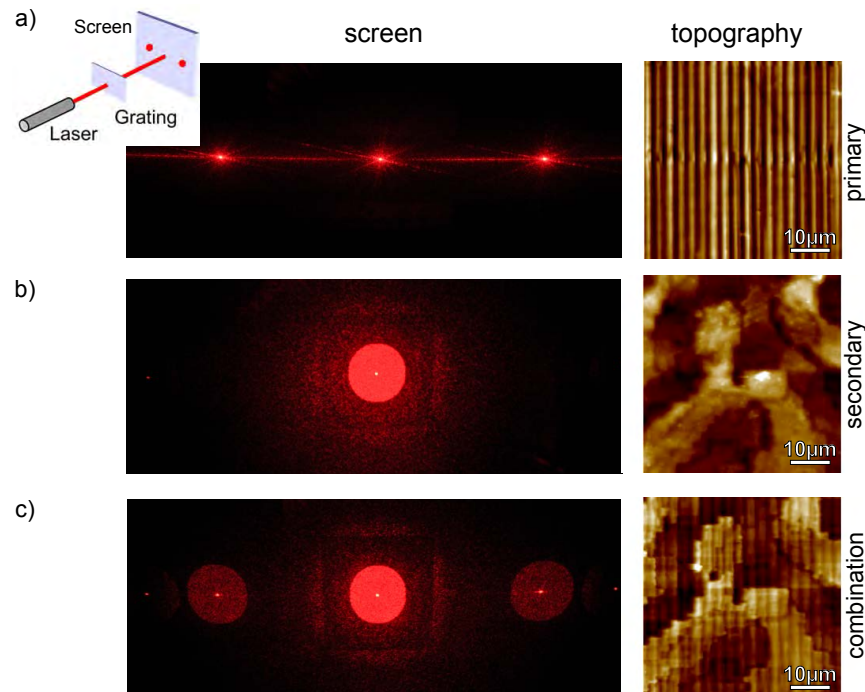


Fig. 4. Combination of two diffractive optical elements. The photos on the left show the image on the screen when the DOEs are illuminated with a laser as depicted in the sketch in the upper left corner. The images in the right column represent the topography of the DOEs measured by atomic force microscopy. (a) The linear grating results in a characteristic interference pattern. (b) The PF-DOE creates a flattop as diffraction pattern. (c) The superposition of both optical structures creates a combined pattern, i.e., the flattop appears as main and side order of the linear grating.

3. Conclusion

These examples prove the feasibility of the overall concept and give a prospect on the potential of the achievable complexity using nano- and microthermoforming with active SMP molds. In contrast to other techniques it allows the replication of complex, hierarchical optical structures with undercuts on large areas. However, the combination of two polymers into the final product implies certain restrictions regarding their properties. The glass transition temperature T_g of the polymer employed as the thin covering film has to lie between the transition T_{trans} and the permanent temperature T_{perm} of the SMP. This choice ensures the recovery of the permanent shape of the SMP at the glass temperature during the thermoforming step. Furthermore, the

hot embossing of the thin film has to be performed at or above its glass transition temperature but not above the permanent temperature of the SMP as this would erase the permanent shape. Since the transition and the permanent temperature depend on the actual SMP the previously mentioned adaptations represent no limitation of the process itself but they are an important point of consideration for the choice of the spin-coated polymer.

The use of shape memory polymers as active mold inserts has several advantages compared to classical microthermoforming where a gas is used to press the polymer film into the cavities of the mold. Small holes and/or ruptures of the film can lead to a loss of pressure and ultimately to imperfect results as well as further cracks in the film. In the presented process, the SMP effectively replaces the pressurized gas by its ability to recover to its pre-structured form, thus forming the thin covering polymer film into its final shape. Since the SMP remains in a rubber-like elastic state rather than melting entirely, holes in the polymer film do not result in pressure loss. Consequently, overcoming this basic limitation allows also thermoforming of deliberately perforated films like permeable membranes.

Furthermore, as the polymer foil adheres strongly to the SMP, its uniform heating is improved. In classical thermoforming the high surface to volume ratio of thin foils demands longer process times to ensure a uniform temperature since the in-plane heat distribution is severely hampered. In addition, a precise temperature control is mandatory to compensate for the strong coupling of the foil to the surrounding environment. However, in the presented process the SMP acts as an additional medium for the heat transfer and as a heat reservoir to compensate for possible temperature fluctuations during the final thermoforming step.

So far we produced samples with diameters of about 5 cm in a controlled and reproducible way. Using commercial hot embossing or nanoimprint machines it will be straightforward to extend this value to 8" and to produce large areas with complex hierarchical nano- and microstructures. Nonetheless, even larger areas seem feasible as hot embossing can be extended to a roll-to-roll process [30]. The crucial point for this up-scaling is the drying or baking of the thin film on top of the SMP. This issue, however, might be solved by moderate heating and vacuum drying. Consequently, active molds made from SMPs are a promising approach for the mass production of complex, hierarchical optical structures.

Acknowledgments

N. S. acknowledges financial funding by the Helmholtz International Research School for Teratronics. We thank Radwanul Siddique, Senta Schauer, Tobias Meier, and Richard Thelen (KIT) for their kind support and helpful discussions. This work was partly carried out with the support of the Karlsruhe Nano Micro Facility (KNMF, www.kit.edu/knmf), a Helmholtz Research Infrastructure at Karlsruhe Institute of Technology (KIT, www.kit.edu).